Equation of state of model branched alkanes: Theoretical predictions and configurational bias Monte Carlo simulations

Luis G. MacDowell,[a] Carlos Vega, and Eduardo Sanz
Departamento de Química Física, Facultad de Ciencias Químicas, Universidad Complutense,
Madrid 28040, Spain

We develop a general configurational bias Monte Carlo algorithm for the simulation of branched alkanes and compare the results with predictions from theoretical equations of state. We consider results for all the hexane isomers, as well as for several heptane and octane isomers. The interaction sites of our united atom model alkanes are hard spheres of equal diameter, thus allowing us to study the effect of branching in the equation of state without the need of considering the effect of changes in the size of the sites. We find that, at roughly constant molecular volume, branching has a small but noticeable effect on the equation of state, somewhat reducing the pressure at which a given density may be attained. We find that equations of state previously used for linear chains yield very good agreement with simulation results. © *2001 American Institute of Physics.*
[DOI: 10.1063/1.1397332]

I. INTRODUCTION

Our knowledge on the equation of state (EOS) of flexible chain molecules has very much improved in the last 15 years. The earlier studies in this area were concerned with rather idealized chain molecules, made of tangent hard spheres. A very important advance was the formulation of a (first-order) thermodynamic perturbation theory (TPT1), which allowed to express the properties of the chain molecules in terms of the properties of the constituent monomers.[1–5] Other accurate theories for tangent hard spheres, such as the Generalized Flory Dimer (GFD)[6,7] or a recent theory by Lue (LT)[8] have also been proposed. As an important difference with respect to TPT1, these theories require either single chain properties (GFD) or two chain properties (LT) as an input.

Considering the importance of branched molecules, it is not surprising that all of these theories have been extended to predict the properties of star polymers. In fact, to first order the thermodynamic perturbation theory of Wertheim predicts that the equation of state of a star polymer is equal to that of a linear chain with the same number of monomers.[9] This hypothesis was shown to be very accurate in a simulation study by Yethiraj, who also extended GFD to star polymers with good results.[10] Similar conclusions, both from theory and simulation are also found by Patrickios and Lue.[11]

A rather more difficult problem arises when one tries to describe the equation of state of more realistic molecular models, with chemical features such as overlapping interaction sites, fixed bending angles, and torsional barriers. Most frequently, the equation of state of such models is obtained as an empirical modification of the more soundly based equations of state of tangent hard spheres. As an example,

several authors have proposed to describe chains of overlapping hard spheres by using an effective number of tangent spheres into the original TPT1 equation of state.[12–16] Our own work shows that one such variant, which we call modified Wertheim theory (MW1), describes very accurately the equation of state of linear alkanes with up to 30 carbon atoms.[17–19] Similarly, Hall and co-workers have extended the original GFD in several different ways to account for chain overlap[7,20,21] and Mehta and Honnell[22] have shown that good agreement with hard *n*-alkane models of up to eight carbon atoms may be obtained.

Now, when it comes to consider realistic models of repulsive branched alkanes, then the situation is far less satisfactory, as both theoretical and simulation studies are very scarce if existent. The importance of having accurate equations of state for realistic repulsive models should not be overlooked, as such a knowledge is essential in a perturbation theory for realistic model alkanes with attractive interactions. Indeed, the availability of reasonably good equations of state for repulsive *n*-alkanes has allowed to study the equation of state of real alkanes with attractive interactions.[23–26] As an example, we have recently added a simple mean-field perturbation term to our MW1 equation of state and found that this approach is able to describe important qualitative features of *n*-alkanes.[27] Using a somewhat more elaborated theory, we studied the critical properties of branched alkanes and found good qualitative agreement.[28] Recent advances using the Polymer Reference Interaction Site Model (PRISM) have also been reported.[29]

The simulation of branched alkanes is already by its own a rather interesting issue that has attracted much attention.[30–34] Initially, such simulations were usually performed using molecular dynamics. However, as new sampling techniques were introduced[35] and the configurational bias method was developed,[36–38] Monte Carlo simulations became the preferred choice, specially when phase equilibria

---
[a]Present address: Institut für Physik (WA31), Johannes Gutenberg Universität, 55099, Mainz, Germany. Electronic mail: luis.macdowell@uni-mainz.de

was a matter of concern.[39–42] The extension of configurational bias to branched alkanes, however, might not be as straightforward as one could expect at first thought. The reason is that in such case, not all of the torsional and bending potential terms may be written as functions of a single generalized coordinate. Accordingly, sampling of trial positions from canonical distributions of bending and torsional potentials becomes much more involved. This fact was probably first realized by Dijkstra[31] and then considered in more detail by several authors.[32–34] In this work we will overcome all the difficulties related with sampling of the generalized degrees of freedom by simply freezing all of the bending angles to their equilibrium positions. Note that the whole description of the intra-molecular energy in terms of the bending and torsional potentials relies explicitly in assuming that these terms are separable. Such an approximation, on its turn, relies in assuming that bending is subject but to small fluctuations. Accordingly, assuming constant bond angles is then rather reasonable, as long as the Hamiltonian of the alkanes may be described in terms of uncoupled bending and torsional contributions.

The goal of this paper is therefore twofold. First, we will try to fill the lack of simulation results for repulsive model branched alkanes. Second, we will show that straightforward extensions of theories previously used for n-alkanes afford a good description of the equation of state.

The rest of the paper is organized as follows: In next section we present our model and the classical flexible constraint approximation for branched alkanes. Section III is devoted to the simulation technique and methodology. In Sec. IV we describe two modifications of Wertheim's TPT1 for branched alkanes and compare them with simulations in Sec. V. We then present our conclusions.

II. MODEL, GENERALIZED COORDINATES, AND FLEXIBLE CONSTRAINTS

A. Classical model for branched alkanes

The alkane model that will be employed may be considered as a straightforward extension of the repulsive united atom n-alkane model that was employed in previous work.[17,18]

Each of the CH_n groups that may be found in a branched alkane is described by a single hard sphere interaction site of diameter $d = 3.7109$ Å. Obviously, a more realistic model would account for interaction sites of different size, but here we will concentrate on the effect of branching. It is, therefore, convenient to consider identical interaction sites, so that addition of different branches has very little effect on the overall molecular volume.

We will consider that the hard-sphere potential is responsible for all of the intermolecular interactions and for those intramolecular interactions which take place between atoms more than three bonds apart. Bond distances and bond angles will be described by means of harmonic potential wells whose force constants are considered to be infinitely large. Effectively, this corresponds to fixing the bond distance and angles to their equilibrium values, which we will set to $l_0 = 1.53$ Å and $\theta_0 = 109.47°$, respectively.

The flexible nature of the molecule will be introduced at the level of the torsional degrees of freedom. In this work, we will consider the simplest approximation, so that the overall potential about a given bond vector is considered to be the sum of n-butane torsional potentials. More specifically, we will consider that the potential that governs the motion of the chain about a given bond vector, say, that bond vector formed by atoms i and $i+1$, is

$$U_{\text{tor}} = \sum u_{\text{tor}}(\varphi_k), \tag{1}$$

where the sum extends over all the dihedral angles formed between the atoms bonded to i and the atoms bonded to $i+1$. Furthermore, u_{tor} is an elementary n-butane torsional potential, which we consider to be of the Ryckaert–Bellemans type.[43] Within this approximation, it may be shown that there are a total of six classes of torsional potentials, depending on the local architecture about the considered bond vector (see Fig. 1). Furthermore, depending on the orientation (chirality) of the branches relative to the main chain, subtypes of these six main classes may appear. Table I shows all of the possible torsional potentials that may be found for the six architectures of Fig. 1, expressed in terms of the n-butane elementary potentials. In order to explain all the possible situations, we introduce the phase, Δ. This variable tells us which is the dihedral angle of a branch bonded to atom 3 when the main chain, 1-2-3-4, is in the *trans* conformation (see Fig. 1). Similarly, Δ' tells us the dihedral angle of a branch bonded to atom 2 as measured relative to the 4-3-2-1 sequence in the *trans* conformation. Furthermore, Δ_k represent the absolute values of such angles. Subscripts "t" and "q" indicate whether the branches considered are attached to a tertiary or a quaternary atom, respectively. For the model considered in this work, where all the bond angles are equal and set to the tetrahedral value, $\Delta_t = \Delta_q = 120°$ (see the Appendix for an expression of Δ_k in terms of bond angles). Although there appear to be 10 torsional potentials, subtypes within a class are related by simple symmetry operations, as follows:

$$U_3(\phi) = U_2(\phi + \Delta_t), \tag{2}$$

$$U_6(\phi) = U_5(\phi - \Delta_t), \tag{3}$$

$$U_7(\phi) = U_5(\phi + \Delta_t), \tag{4}$$

$$U_9(\phi) = U_8(\phi + \Delta_t). \tag{5}$$

In our model, U_8 is a function of period 120°, so that U_8 and U_9 become identical. Also note that the symmetry properties shown above should also hold in more elaborated models where the elementary torsional potentials depend on the molecular architecture.[33]

B. Generalized coordinates

In order to consider the effect of freezing the bond distances and angles to their equilibrium value, it will prove convenient to describe the state of our alkane model in terms of generalized coordinates, consistent with the Hamiltonian described in the previous section. The internal state will be given by a set of hard coordinates, which are those governed
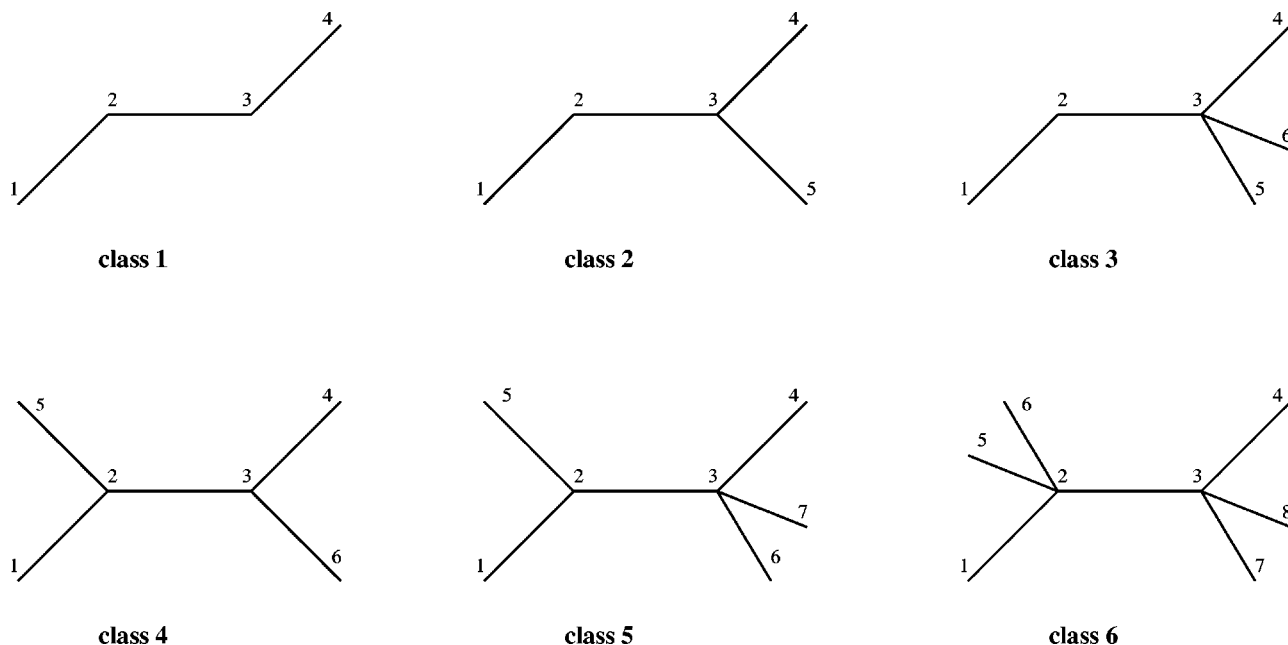
FIG. 1. Sketch of the six possible architectures about a bond vector that may be found in branched alkanes.

by infinitely stiff harmonic potentials (i.e., bond distances and bond angles), and a set of soft torsional degrees of freedom. To be specific, let the alkane have n united carbon atoms and r branches. Also, let us define ''branched-atom'' as the first atom of a given branch. Then, each of the branch atoms will be described by a bond length and the two bond angles formed between that atom and the backbone. On the other hand, each of the remaining non branched atoms will be described by one bond length, one bond angle and one torsional degree of freedom. Accordingly, the set of hard coordinates will consist of $(n-1)$ bond lengths and $(n-2+r)$ bond angles, while the set of soft variables will be the $(n-3-r)$ remaining torsional degrees of freedom.

Once the internal state of the molecule is defined by means of a vector with the hard degrees of freedom, $\mathbf{q}_h$, and a vector with the soft degrees of freedom, $\mathbf{q}_s$, we will consider a vector, $\mathbf{q}_e$, that contains the set of external coordinates. These are, namely, a set of three Cartesian coordinates specifying the position of the first atom, and three Euler

angles specifying the orientation of the three first atoms of the chain relative to a laboratory reference frame.

C. Configurational integral

Once the generalized coordinates have been defined, let us consider the configurational integral of a fluid of N alkane molecules. Most generally, it can be expressed in terms of Cartesian coordinates as follows:

$$Z \propto \int e^{-\beta U} d\mathbf{r}_{11} \cdots \mathbf{r}_{n1} \cdots \mathbf{r}_{nN}, \qquad (6)$$

where U is the total potential energy of the system and $\mathbf{r}_{ij}$ is the vector of Cartesian coordinates of atom i of molecule j. In our case, however, it is far more convenient to express the partition function in terms of generalized coordinates as follows:

TABLE I. List with all the possible torsional potentials of branched alkanes that may be found when expressed in terms of elementary n-butane contributions. See Sec. II A for more details.

Class	Subtype	n^{er} of 1–4 interactions	Chirality
class 1	$U_1(\phi) = u_{tor}(\phi)$	1×1	
class 2	$U_2(\phi) = u_{tor}(\phi) + u_{tor}(\phi - \Delta_t)$	1×2	$\Delta = -\Delta_t$
	$U_3(\phi) = u_{tor}(\phi) + u_{tor}(\phi + \Delta_t)$	1×2	$\Delta = \Delta_t$
class 3	$U_4(\phi) = u_{tor}(\phi) + u_{tor}(\phi + \Delta_q) + u_{tor}(\phi - \Delta_q)$	1×3	
class 4	$U_5(\phi) = 2u_{tor}(\phi) + u_{tor}(\phi + \Delta_t) + u_{tor}(\phi - \Delta_t)$	2×2	$\Delta = -\Delta'$
	$U_6(\phi) = u_{tor}(\phi) + 2u_{tor}(\phi - \Delta_t) + u_{tor}(\phi - 2\Delta_t)$	2×2	$\Delta = \Delta' = -\Delta_t$
	$U_7(\phi) = u_{tor}(\phi) + 2u_{tor}(\phi + \Delta_t) + u_{tor}(\phi + 2\Delta_t)$	2×2	$\Delta = \Delta' = \Delta_t$
class 5	$U_8(\phi) = u_{tor}(\phi) + u_{tor}(\phi + \Delta_q) + u_{tor}(\phi - \Delta_q)$ $+ u_{tor}(\phi - \Delta_t) + u_{tor}(\phi + \Delta_q - \Delta_t) + u_{tor}(\phi - \Delta_q - \Delta_t)$	2×3	$\Delta' = -\Delta_t$
	$U_9(\phi) = u_{tor}(\phi) + u_{tor}(\phi + \Delta_q) + u_{tor}(\phi - \Delta_q)$ $+ u_{tor}(\phi + \Delta_t) + u_{tor}(\phi + \Delta_q + \Delta_t) + u_{tor}(\phi - \Delta_q + \Delta_t)$	2×3	$\Delta' = \Delta_t$
class 6	$U_{10}(\phi) = 3u_{tor}(\phi) + 3u_{tor}(\phi + \Delta_q) + 3u_{tor}(\phi - \Delta_q)$	3×3	

$$Z \propto \int J(\mathbf{q}^N) e^{-\beta U(\mathbf{q}^N)} d\mathbf{q}^N, \tag{7}$$

where $J(\mathbf{q}^N)$ is the Jacobian of the transformation and $\mathbf{q} = (\mathbf{q}_e, \mathbf{q}_s, \mathbf{q}_h)$ is a vector that contains all of the generalized coordinates of one molecule. For the simple case of n-alkanes, it is well known that the Jacobian only depends on the hard and external coordinates of the molecule.[44] In the context of the flexibly constrained model, where the potentials that govern the hard variables are infinitely stiff, this means that all of the hard variables may be trivially integrated out, leaving a configurational integral that only depends on the soft and external degrees of freedom

$$Z \propto \int e^{-\beta \tilde{U}(\tilde{\mathbf{q}}^N)} d\tilde{\mathbf{q}}^N, \tag{8}$$

where $\tilde{U}$ stands for that part of the potential that does not contain hard contributions, while $\tilde{\mathbf{q}} = (\mathbf{q}_e, \mathbf{q}_s)$ is a vector that only contains the external and soft coordinates of a molecule.

For the above equation to hold in the more general case of branched alkanes, it is required to show that the Jacobian of the transformation is also independent of the soft variables. In the Appendix we show that indeed the Jacobian of the transformation from Cartesian coordinates to the set of generalized coordinates does only depend on the hard degrees of freedom. Accordingly, Eq. (8) is the general expression for the partition function of arbitrary branched alkane models within the flexible constraint approximation.

III. SIMULATION METHODOLOGY

In order to calculate the exact equation of state for our model alkane, we will use the well known Monte Carlo technique.[45] In this method, one calculates the average properties of a system by sampling configurations from the probability density, f, consistent with the thermodynamic ensemble considered. First, one attempts to generate a new representative configuration by choosing it from some arbitrary trial probability density, $T(\mathsf{n}|\mathsf{o})$, which determines the likelihood of attempting to generate state n given that the system is in state o. The trial configuration is then accepted with probability

$$A(\mathsf{n}|\mathsf{o}) = \min\left(1, \frac{T(\mathsf{o}|\mathsf{n})f(\mathsf{n})}{T(\mathsf{n}|\mathsf{o})f(\mathsf{o})}\right). \tag{9}$$

A. General configurational bias sampling

Usually, the new state generated differs from the original state only by changes of a small subsystem described by a subset of the complete set of degrees of freedom. In many circumstances, the energy of this subsystem (including interactions with the rest of the system) may be written in terms of a sum of energy terms that may be attributed to different fragments, say, 1 to m

$$U^{\mathrm{sub}} = u_1(\mathbf{b}_1) + u_2(\mathbf{b}_2, \mathbf{b}_1) + \cdots + u_m(\mathbf{b}_m, \mathbf{b}_{m-1}, ..., \mathbf{b}_1), \tag{10}$$

where $\mathbf{b}_i$ is a vector of generalized coordinates that specify the position of fragment i. One typical example of such a situation is a system of alkanes, with the subsystem chosen

to be one given molecule or part thereof; and the fragments the set of monomers within that molecule. In the most general case, when the subsystem is a whole molecule, $\mathbf{b}_1$ is a vector with the Cartesian coordinates of the first atom, $\mathbf{b}_2$ is a vector with two polar angles specifying the orientation of the second atom, $\mathbf{b}_3$ is the third Euler angle specifying the orientation of the third atom and the remaining $\mathbf{b}_{i>3}$ are torsional angles.

A particularly convenient choice for the trial probability density in this situation is known as configurational bias sampling.[36–38] In this technique, one would like to choose trial states for the generalized coordinates of the subsystem, $\mathbf{b}_1 \cdots \mathbf{b}_n$, by sampling each of the vectors, $\mathbf{b}_l$, from a Boltzmann distribution of the corresponding u_l energy term. To be more specific, one would like to select a trial value for $\mathbf{b}_1$ by sampling from the distribution

$$t_1(\mathbf{b}_1) = \frac{e^{-\beta u_1(\mathbf{b}_1)}}{\int e^{-\beta u_1(\mathbf{b}_1')} d\mathbf{b}_1'}, \tag{11}$$

once $\mathbf{b}_1$ is chosen, a trial value for $\mathbf{b}_2$ is selected by sampling from

$$t_2(\mathbf{b}_2; \mathbf{b}_1) = \frac{e^{-\beta u_2(\mathbf{b}_2, \mathbf{b}_1)}}{\int e^{-\beta u_2(\mathbf{b}_2', \mathbf{b}_1)} d\mathbf{b}_2'}. \tag{12}$$

Note that t_2 is a function of $\mathbf{b}_2$ but depends parametrically on $\mathbf{b}_1$. More generally, for fragment l, one selects $\mathbf{b}_l$ by sampling from a Boltzmann distribution of the form

$$t_l(\mathbf{b}_l; \mathbf{b}_{l-1}, ..., \mathbf{b}_1) = \frac{e^{-\beta u_l(\mathbf{b}_l, \mathbf{b}_{l-1}, ..., \mathbf{b}_1)}}{\int e^{-\beta u_l(\mathbf{b}_l', \mathbf{b}_{l-1}, ..., \mathbf{b}_1)} d\mathbf{b}_l'}. \tag{13}$$

It then follows that the overall trial probability density for the chosen subsystem is given as the product of the different t_l

$$T(\mathsf{n}|\mathsf{o}) = \prod_{l=1}^{m} t_l(\mathbf{b}_l; \mathbf{b}_{l-1}, ..., \mathbf{b}_1). \tag{14}$$

The resulting overall acceptance probability is then

$$A(\mathsf{n}|\mathsf{o}) = \min\left(1, \frac{Q_1 \cdot Q_2(\mathbf{b}_1^{\mathsf{n}}) \cdots Q_m(\mathbf{b}_{m-1}^{\mathsf{n}}, ..., \mathbf{b}_1^{\mathsf{n}})}{Q_1 \cdot Q_2(\mathbf{b}_1^{\mathsf{o}}) \cdots Q_m(\mathbf{b}_{m-1}^{\mathsf{o}}, ..., \mathbf{b}_1^{\mathsf{o}})}\right), \tag{15}$$

where the Q_l factors represent the integrals in the denominators of Eqs. (11)–(13), while the superscript n stands for the new attempted state and the superscript o stands for the actual state of the system.

In order to get further physical insight into the problem, it will prove convenient to rewrite the Q_l integrals. Without loss of generality, consider that each of the energy terms of Eq. (10) may be expressed as two separated contributions

$$u_l(\mathbf{b}_l, \mathbf{b}_{l-1}, ..., \mathbf{b}_1) = u_l^{\mathrm{int}}(\mathbf{b}_l) + u_l^{\mathrm{ext}}(\mathbf{b}_l, \mathbf{b}_{l-1}, ..., \mathbf{b}_1), \tag{16}$$

where u_l^{int} is some stiff potential, which restricts the degrees of freedom of fragment l to a narrow region; while u_l^{ext} is some softer potential, with shallower potential minima. For example, in our model alkane the stiff potential is that which governs the torsional motion, while the loose potential is that of the hard-sphere interactions, both intra and intermolecular. Whereas the labeling of these two energy contributions has

been made in terms of the physical characteristics of the potential, note, however, that what is really relevant here are their mathematical characteristics: u_l^{int} must only depend on b_l, while u_l^{ext} may depend on all of the degrees of freedom of u_l. With this division, one can show that the Q_l integrals may be written as follows:

$$Q_l(\mathbf{b}_{l-1},\ldots,\mathbf{b}_1)=C_l\int e^{-\beta u_l^{\text{ext}}(\mathbf{b},\mathbf{b}_{l-1},\ldots,\mathbf{b}_1)}\frac{e^{-\beta u_l^{\text{int}}(\mathbf{b})}}{C_l}\,d\mathbf{b},$$ (17)

where C_l is an integral over the Boltzmann factor of the stiff potential

$$C_l=\int e^{-\beta u_l^{\text{int}}(\mathbf{b})}d\mathbf{b}.$$ (18)

Note that it is understood that when $l=1$, the list of arguments $\mathbf{b}_{l-1},\ldots,\mathbf{b}_1$ in Eq. (17) may be ignored. This also holds for Eqs. (19) and (20) below. From Eq. (17) one can immediately see that Q_l may be considered as an average of the Boltzmann factor of the loose potential over the canonical probability density of the stiff potential[46]

$$Q_l(\mathbf{b}_{l-1},\ldots,\mathbf{b}_1)=C_l\langle e^{-\beta u_l^{\text{ext}}(\mathbf{b},\mathbf{b}_{l-1},\ldots,\mathbf{b}_1)}\rangle_{\text{int}}.$$ (19)

We now introduce (continuum) Rosenbluth factors, defined as:

$$\widetilde{w}_l=\langle e^{-\beta u_l^{\text{ext}}(\mathbf{b},\mathbf{b}_{l-1},\ldots,\mathbf{b}_1)}\rangle_{\text{int}}.$$ (20)

In terms of these factors, one can then show that the appropriate acceptance rule consistent with the attempt probability of Eqs. (11)–(13) is

$$A(\mathsf{n}|\mathsf{o})=\min\left(1,\frac{\widetilde{w}_1\cdot\widetilde{w}_2(\mathbf{b}_1^{\mathsf{n}})\cdots\widetilde{w}_m(\mathbf{b}_{m-1}^{\mathsf{n}},\ldots,\mathbf{b}_1^{\mathsf{n}})}{\widetilde{w}_1\cdot\widetilde{w}_2(\mathbf{b}_1^{\mathsf{o}})\cdots\widetilde{w}_m(\mathbf{b}_{m-1}^{\mathsf{o}},\ldots,\mathbf{b}_1^{\mathsf{o}})}\right).$$ (21)

In practical situations, however, it is not possible to evaluate the Rosenbluth factors of Eq. (20) exactly, while sampling from the continuous attempt probabilities of Eqs. (11)–(13) is also very difficult, as the Q_l are not known. Actually, selection of a trial value for the fragments, say, fragment l, proceeds as follows. First, one chooses a set of k possible positions for vector $\mathbf{b}_l$, sampled from a canonical distribution of the stiff potential ($\propto e^{-\beta u_{\text{int}}}$). The trial position for the fragment, $\mathbf{b}_l^t$ is then selected among these finite set of possible positions from a discrete probability distribution of the form

$$t_l(\mathbf{b}_l^t)=\frac{e^{-\beta u_l^{\text{ext}}(\mathbf{b}_l^t)}}{\sum_{j=1}^k {}^* e^{-\beta u_l^{\text{ext}}(\mathbf{b}_l^j)}}.$$ (22)

If we now impose super detailed balance, that is, detailed balance between "super states," defined as a canonical state together with its set of $k-1$ possible positions for each vector $\mathbf{b}$, it follows that the acceptance rule is formally as in Eq. (21). The only difference is that the exact continuous Rosenbluth factors are substituted by their approximate, discretized counterparts

$$w_l=\frac{1}{k}\sum_{j=1}^k {}^* e^{-\beta u_l^{\text{ext}}(\mathbf{b}_l^j)},$$ (23)

where the asterisk next to the sum in the two previous equations reminds that the $\mathbf{b}_l^j$ positions are chosen from the canonical distribution of the stiff potential.

One subtlety of this approach is that by imposing super detailed balance, one is no longer sampling from the canonical distribution, but from an extended or "super canonical" distribution of the form

$$\hat{f}(\mathbf{q}^N,\mathbf{S}^N)=f(\mathbf{q}^N)\cdot g(\mathbf{S}^N),$$ (24)

where $\mathbf{S}^N$ is the set of vectors with $k-1$ "dummy" possible positions for each degree of freedom, while g is their probability distribution. Actually, this has no practical significance whatsoever, as $f(\mathbf{q}^N)$ and $g(\mathbf{S}^N)$ are completely independent. For this reason, the long term average over the dummy variables, $\mathbf{S}^N$, yields unchanged the desired canonical distribution. In this way, it is seen that continuum configurational bias may be considered as one of the modern extended ensemble simulation methods.[47]

In this section we have gone through a rather formal description of the configurational bias method somewhat based on ideas by Maginn et al.[46] The reason is that we wanted to stress the generality of the technique, which is applicable to any system whose potential energy may be written as in Eq. (10). The concept of super detailed balance required to justify the extension of configurational bias to continuum systems was first introduced by Frenkel et al.[38] and is further discussed in a recent book with emphasis in the actual implementation of the algorithm.[48]

B. Technical details

As seen in the previous section, there is no formal difference between simulating branched and linear alkanes, as long as their Hamiltonian is expressed in accordance with Eq. (10). Technically, however, some difficulties appear when (i) calculating the coordinates, when (ii) evaluating the energy, and when (iii) sampling the torsional angles. We consider each of these in turn.

1. Choosing a growth path

The first problem that arises when considering a branched alkane is exactly how to label the different atoms. This we do by following the conventions that are used in organic chemistry to name an alkane.[49] In this way, it is found that the structure of an alkane may be completely specified from the order of the branches,[50] the number of branches of each order, the number of atoms in each branch and the label of the atoms to which they are attached. Note, however, that this procedure does not provide a unique way of characterizing the alkane. Indeed, there may be many several such sets of data which specify the same alkane (e.g., isopentane may be considered to be either 3-methylbutane, 2-methylbutane, or 2-ethylpropane). Each of the possible ways of specifying an alkane in this way, by choosing arbitrarily one terminal atom as the first one and other terminal atom as the last one, we call it a *complete growth path*. Actually, as the atoms are labeled, it is found that the total number of complete growth paths is $n_{\text{ends}}(n_{\text{ends}}-1)$, where n_{ends} is the number of ends of the molecule. In practice, it is well known that complete regrowth of a chain molecule in a
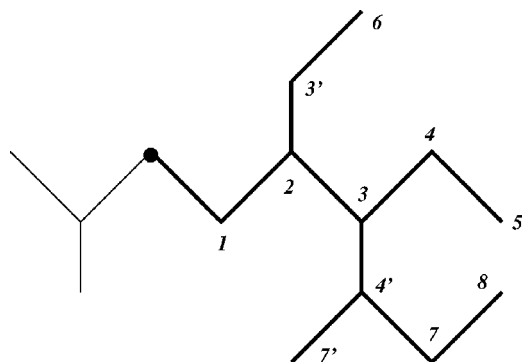
FIG. 2. Choosing a growth path. The black circle shows the tagged atom, chosen at random among all the atoms. The bold lines show the fragment of the chain that is selected for regrowth. The numbers represent the number of iterations in the algorithm (see text) and also serve here to label the atoms. Atoms 1 and 2 are selected first. At 2, a branch point is encountered. 3 is selected as "next" atom, and $3'$ as the first atom of the next branch. The growth then continues to atom 3, where 4 is selected as next atom and $4'$ as the first atom of the next branch (this puts the counter of branches of higher order to two). Iterations of the inner loop end at atom 5. As there are no branches of current order left, the algorithm proceeds to consider branches of the order above (note that, during regrowth and retracement, atoms i and i' are grown simultaneously).

fluid may be very difficult, so we not always attempt regrowth along a complete growth path, but also allow for regrowth along a part thereof. Any possible such part, including complete growth paths is called a *growth path*.[51]

In order to select just any of these possible growth paths with equal probability, we use a set of pointers which allow to specify which are the atoms bonded to a given atom. We use a Verlet list like structure to book this information at the beginning of the simulation.[52] We then proceed in the following way: First, we tag at random one atom of the chain, which will eventually become the first "root" atom (see below). We then choose randomly one out of all the atoms attached to this tagged atom to become the first atom of the branch to be grown. All the remaining atoms bonded to the tagged atom are considered to belong to branches of lower order and will be left unchanged. The branch to be grown is thus the first "child" branch of current order and the only child branch of the lower order branches.

Once these preliminary definitions are made, a whole (random) growth path may be now generated by going through the following iterative scheme (see Fig. 2, for an example):

(1) Let the first child branch of current order become the "current" branch;

(2) let the first atom of the current branch become the current atom and let the atom of the parent branch to which it is bonded become the root atom;

(3) out of all the atoms bonded to the current atom (less the root atom), choose a new atom and let this be the "next" atom;

(4) let all the atoms bonded to the current atom (less the root and next atoms) be stored as first atoms of branches of higher order and recall the label of the current atom;

(5) let the current atom become the root atom. Also let the next atom become the current atom;

(6) repeat from step 3 as many times as required, until a CH_3 atom is encountered and the end of the current branch is, therefore, reached;

(7) if any branch of current order remains to be considered, let the first of these become the current branch and go to step 2. Otherwise continue below;

(8) if branches of higher order remain to be considered, let the next order become the current order and go to step 1. Otherwise end.

Figure 2 shows an example of this algorithm in action for a heavily branched alkane. Note that the above iterative procedure consists mainly of three nested loops. The first one controls the number of generations, or orders of the branches. The second one controls the number of branches of each generation and the third one controls the number of atoms per branch. The outcome of such an algorithm is a list with all the structural information required to grow the chosen fragment, namely, number of branches per order, number of atoms per branch and label of the atom to which branches are bonded, as well as a list with the label of the atom to be grown in the kth place. Other structural properties of the fragment to be regrown, such as the current torsional angles and chirality of the branches may be also calculated while walking along the growth path. Once these properties are known, growth and retracement proceeds by using a similar iterative procedure which is much simpler because the number of iterations that must be performed in each loop is now known (i.e., the repeat-until loops that appear in the previous algorithm are replaced by do loops with bounds that were determined while choosing the growth path).

Note, however, that one must grow at once all of the atoms of one branch, say branch i, together with the first atom of whichever branch attached to i while performing regrowth and retracement. The reason is that the torsional angle right before a root point completely specifies the position of whichever atom is bonded to that root point. Accordingly, the elementary energy term related to this degree of freedom [see Eq. (10)] includes the interactions of all such atoms (see Fig. 2, for an example of the growth order of atoms).

2. Calculation of the coordinates

Now that we have devised a method to randomly select a fragment of the alkane, what is needed is a procedure for the calculation of the actual coordinates. One easy way that has been employed for linear alkanes is by simply specifying the Cartesian coordinates of an atom relative to the previous atom.[40] Such a procedure is very simple, though not necessarily very effective, as the Cartesian coordinates do not appear explicitly in the Hamiltonian. Indeed, this method may cause serious difficulties when applied to branched alkanes.[32–34] For this reason, we choose to characterize the spatial configuration of the alkanes by means of a set of generalized coordinates which are, essentially, a set of torsional angles plus external coordinates. The torsional angles may be sampled easily from the appropriate torsional potentials, as we will explain later. In order to convert the set of generalized coordinates to Cartesian coordinates, we use the

method of rotation matrixes as describes by Flory.[53] In order to extend the method to calculate the Cartesian coordinates of a branched alkane, we simply need to consider it as a bunch of linear atom sequences that bifurcate at the branch points (e.g., 3-methylpentane is considered to be the superposition of a linear chain of five atoms and of other linear chain of four atoms that shares its three first atoms with the previous, longer, chain. Obviously, these three first atoms need not be recalculated). Thus, when calculating the coordinates of the current branch, one just needs to remember the rotation matrix used to grow the first atom of each of the branches attached to it. Subsequent regrowth of these higher-order branches may be then performed as in a linear chain, by employing the previously stored rotation matrix to begin with.

3. Evaluation of the energy

We find it convenient to evaluate the intra and intermolecular energies separately. The reason is that, contrary to the case of linear alkanes, there is no clear way of determining whether two atoms of the same chain are more than three bonds apart from knowledge of their labels (assigned as described previously) alone. In order to be able to take this decision right away during run time, an intra-molecular Verlet neighbor list is created at the beginning of the simulations. This list specifies, for each of the atoms of the chain, which other atoms of that chain are more than three bonds apart. This list is created once and for all and needs not be updated.

As to the intermolecular interactions, we use a linked cell list method.[52] Contrary to the more conventional approach, however, we allow the cells to become smaller than the range of the potential. Actually, we fix the number of cells, not their length. This allows to employ the method at high densities and to extend it to the NpT ensemble, where the volume of the simulation box changes. In order to avoid counting intra-molecular interactions two times, each time the energy of a molecule is being evaluated, we take it out of the list, and then include it again, presumably updated, after the attempted Monte Carlo (MC) move.

4. Sampling of the torsional angles

In most previous configurational bias Monte Carlo applications to branched alkanes, the models employed had explicit torsional and bending potentials. This introduces an important complication, because in this case more bond and torsional angles appear than there are degrees of freedom. In this situation, sampling of the degrees of freedom from the stiff bending and torsional potentials becomes a major complication. At least three different ways of tackling the problem have been considered.[32–34]

In the case of the model alkane proposed here, the situation is much simpler, because all of the bond angles have been frozen. Accordingly, the only remaining internal degrees of freedom are the torsional angles. More importantly, to each of these there corresponds a single torsional potential, independent from all the others. In such a situation, the energy of each fragment may be expressed as in Eq. (16) so

that the configurational bias method may be applied in a straightforward manner. Essentially, what is needed is to sample the independent torsional angles from a canonical distribution of the corresponding torsional potential (one out of the 10 possible torsional potentials). The most popular way of sampling from this sort of distribution is known as the (Boltzmann) rejection scheme.[48,54] For very narrow probability distributions, as is the case of branched alkanes or even linear alkanes at low temperature, this method becomes highly inefficient, to such a point that acceptable trial position sampling may become the rate determining step in simulations.[33] In order to avoid this difficulty, we have considered the transformation method[54] and found it to yield an excellent performance. In the transformation method, one would like to sample a random variable, t, defined in the interval $[a,b]$, from a normalized distribution function, $f(t)$. In order to do so, consider the distribution function, $F(t)$, defined as

$$F(t) = \int_a^t f(x)dx. \tag{25}$$

The desired random variable, t, may be sampled in accordance with $f(t)$, from the following equation:

$$t = F^{-1}(p), \tag{26}$$

where F^{-1} is the inverse function of F and p is a random number between 0 and 1 generated from a uniform distribution.

In order to calculate F^{-1} for use during run time, we proceed as follows:

(i)   Numerically evaluate $F(t)$ for a large number of evenly distributed points between 0 and 2π;
(ii)   generate an interpolating function for $F(t)$, and use it to tabulate F^{-1} for an evenly distributed set of points between 0 and 1;
(iii)   use the tabulated set of data for F^{-1} to generate an interpolation spline polynomial.

Once this polynomial has been calculated, F^{-1} can be used during run time to generate the desired random variable from Eq. (26). We find that the transformation method works very well, provided that a good interpolation function is used for F^{-1}. A simple linear interpolation scheme fails completely, unless F^{-1} is tabulated at a very large number of points. On the contrary, using a standard spline method with 500 evenly distributed points between 0 and 1 already produces an accurate and smooth $f(t)$. In practice, we used 1000 points to generate the spline polynomial in order to be in the safe side.

At first thought, it would appear that an F^{-1} function would have to be created for each of the 10 possible torsional potentials (see Table I). In practice, however, only one F^{-1} function for each of the six classes of torsional potentials needs to be evaluated, as several of the torsional potentials are trivially related by translation [see Eqs. (2)–(5)].

The global strategy that we use for a configurational bias move is as follows: First, we choose randomly one molecule that will be subject to the attempted move. Then, we choose

J. Chem. Phys., Vol. 115, No. 13, 1 October 2001

Equation of state of model branched alkanes   6227

TABLE II. Single chain simulations for selected alkanes. $\langle R^2 \rangle$ is the mean-squared end to end distance (ends of the backbone); $\langle S^2 \rangle$ is the mean squared radius of gyration; n_g is the number of gauche angles and "accept" stands for the acceptance ratio (%). "all-ccb" stands for the configurational bias simulations with all possible growth paths chosen with equal probability. "one-ccb" stands for the CB simulations when growth is performed always along the same complete growth path. The numbers in parenthesis are a measure of the error in the last digit as measured by a single standard deviation. All distances measured in units of the σ parameter of a CH_2 group.

	$\langle R^2 \rangle$	$\langle S^2 \rangle$	n_g	% accept
	3,3-dimethyl-4-ethylhexane			
all-ccb	2.21(4)	0.3412(2)	8.0001(2)	30
one-ccb	2.20(2)	0.3409(3)	8.000(0)	1.4
pivoting	2.23(3)	0.3406(1)	8.0001(1)	32
	4,8-dipropyldodecane			
all-ccb	5.66(1)	1.0086(6)	9.03(1)	56
one-ccb	5.64(1)	1.0091(5)	9.021(6)	31
pivoting	5.62(3)	1.010(1)	9.02(1)	58
	squalane			
all-ccb	15.7(1)	2.44(1)	14.59(1)	37
one-ccb	15.4(1)	2.42(1)	14.59(2)	20
pivoting	15.5(2)	2.41(2)	14.62(3)	58

at random one of all the possible growing paths, which can be either complete (complete growth of the molecule) or partial (growth starts at a given atom chosen at random such that at least one torsional angle is sampled). Finally, retrace and re-growth of the chain is performed along the chosen path and the resulting Rosenbluth factors calculated. For further details and a more detailed account of the simulation procedures employed, the reader is referred elsewhere.[55]

Before closing this section, let us show that the proposed methodology does indeed properly sample the internal degrees of freedom of our model alkanes. In order to do so, we have performed single chain simulations using both configurational bias and the simple pivoting algorithm (random rotations of a part of the chain about a chosen bond vector). Simulations have been performed for three selected alkanes, 2,6,10,19,23-hexamethiltetracosane (squalane), 3,3-dimethyl-4-ethylhexane and 4,8-dipropyldodecane at a temperature of 600 K. As some of these alkanes are rather bulky, we find it necessary to replace the hard-sphere sites with Lennard-Jones sites. The Lennard-Jones parameters used are those proposed by Poncela et al.[56] in order to mimic real alkanes, but all the remaining geometrical parameters and torsional potentials are kept as described before. The results for the mean squared end to end distance, mean squared radius of gyration and number of torsional gauche angles (i.e., those torsional angles lying in the interval $[\pi/3, 5\pi/3]$) are collected in Table II. Note also that two different variants have been employed for the configurational bias simulations. In one variant, sampling proceeds along a single complete growth path chosen a priori (one-ccb). In the other variant, sampling is performed along all the possible growth paths, either complete or partial (all-ccb), chosen randomly with equal probability. As the table shows, both the pivoting and the configurational bias methods yield essentially the same results. Note also that both of the configurational bias variants give the same results. In principle one needs not select at

random the growth paths used to sample the torsional angles. However, always using the same path may result in poor sampling. This can be seen from the results for 3,3-dimethyl-4-ethylhexane, where the acceptance rate along the arbitrarily chosen (complete) growth path is only 1.4%. Allowing for a choice of different growth paths may result in a large increase of the acceptance rate. For this very bulky branched alkane, allowing for a choice of growth paths results in an increase of the acceptance rate of one order of magnitude.

C. Simulations

All of the simulation results were obtained using a cubic box of 108 molecules in the constant pressure (NPT) ensemble. Production runs of 40 000 cycles were preceded by equally long equilibration periods for each thermodynamic state. Each cycle consists of 108 canonical (NVT) trial moves, and one volume change attempt. The NVT moves were chosen in the proportion 5:5:9:1 from the following choices: (1) Center-of-mass translation of the molecule; (2) rotation of the molecule about a randomly chosen axis across an atom of the molecule chosen at random; (3) rotation of one or more torsional angles using configurational bias; (4) full chain re-growth using configurational bias for all the degrees of freedom of the chain. The simulations were started by arbitrarily choosing one molecular conformation and replicating it in space as if it were an α-N_2 lattice. The volume was chosen big enough so as to avoid overlapping. The isotherms were then produced by gradual compression. Some expansion runs were also performed and found to agree with the compression. Due to the use of configurational bias and linked cell lists, the cost of a simulation strongly depends on the state density. Each of the isotherms produced required between 24 and 36 hours of CPU time in a 350 MHz processor, depending on the size of the molecules, but little on the number of branches. Our general MC code has been tested by comparing with the literature for rigid models,[57] flexible hard alkanes,[58,70] soft alkanes,[59] and Lennard-Jones united atom alkanes.[60] Good agreement was found in all cases.

IV. EQUATION OF STATE FOR BRANCHED ALKANES

The first order thermodynamic perturbation theory of Wertheim (TPT1) allows to express the free energy of an associating system in terms of the properties of a reference fluid with no association.[4] When one considers the limit of complete association, TPT1 yields an expression for the equation of state of chain molecules.[5,61] For the case of a fluid made of chains of tangent hard spheres, TPT1 yields[5,9]

$$Z = n \frac{1 + y + y^2 - y^3}{(1-y)^3} - (n-1) \frac{1 + y - y^2/2}{(1-y)(1-y/2)}, \quad (27)$$

where n is the number of tangent hard spheres in the chain, while y is the packing fraction, given as the product of the molecular volume, v_{mol} and the number density, ρ.

This simple equation has been shown to give a rather accurate description of tangent hard spheres.[5] In practice, however, actual molecules are modeled with interaction sites

that overlap considerably, and are known to have rather stiff bond angles and a torsional potential that governs the motion about bond vectors.[53] Whereas the extension of the original TPT1 to such complicated geometries posses yet unsolved problems, a number of empirical modifications of Eq. (27) have been suggested that allow to describe more realistic chain molecules.[12–17] Essentially, all these approaches imply the determination of an effective number of *tangent hard spheres* in terms of geometrical properties of the actual model under consideration.

One such approach is known as the modified Wertheim equation (MW). Here, the effective number of hard spheres is determined in such a way that the actual second virial coefficient of the molecule under consideration is correctly described. The original Eq. (27) is then rewritten as follows:

$$Z = (2\alpha - 1)\frac{1 + y + y^2 - y^3}{(1-y)^3} - (2\alpha - 2)\frac{1 + y - y^2/2}{(1-y)(1-y/2)},$$

(28)

where the nonsphericity parameter, α, is a geometrical property defined in terms of the second virial coefficient of the molecule under consideration

$$B_2/v_{\text{mol}} = 3\alpha + 1.$$

(29)

The advantage of expressing Eq. (28) in terms of α is that it has a rather intuitive interpretation, as it measures to what extent does a molecule deviate from sphericity.

Initially, Eq. (28) was used to describe realistic models of *n*-alkanes up to 8 carbon atoms and shown to give rather satisfactory results.[17] The main drawback of this treatment is that, for long chains, the computation of B_2 may become rather time consuming. To avoid this difficulty, we have proposed a method based on convex body geometry (CBG) that allows to give very accurate estimates of B_2 for chains of up to 100 interaction sites, as well as for models of branched alkanes.[18,62] When this method is used to determine B_2, it can be shown that Eq. (28) yields a very good description of model *n*-alkanes of up to 30 carbon atoms.[18] For details of the method, the reader is referred to the original papers.[18,62] Here, it suffices to say that the proposed methodology allows to determine B_2 from knowledge of single chain properties alone, namely, the surface, volume, and principal moments of inertia. Other required geometrical properties, such as the volume and surface of each conformer may be calculated using an algorithm due to Dodd and Theodorou.[63]

Another empirical modification of Eq. (27) was suggested by Zhou, Hall, and Stell.[16] These authors determine the number of effective tangent hard spheres of the chain in such a way that the effective fluid has the same surface and volume as the molecules under consideration. It then follows that the effective number of tangent hard spheres is given by:

$$n_{ef} = \frac{s_{\text{mol}}^3}{36\pi v_{\text{mol}}^2},$$

(30)

where s_{mol} is the surface of the molecule under consideration.

In order to facilitate subsequent discussion, it is convenient to keep the form of the original MW equation [Eq. (28)]. When this is done, the Zhou–Hall–Stell methodology

for the prediction of the number of effective tangent hard spheres amounts to the following alternative definition for α:

$$\alpha = \frac{1}{2}\left(\frac{s_{\text{mol}}^3}{36\pi v_{\text{mol}}^2} + 1\right).$$

(31)

In the next section, we will test the performance of the MW equation of state [Eq. (28)] when applied to the description of branched model alkanes. We will refer to MW1 when the definition of α is as in Eq. (29), and to MW2 when the definition of α is as in Eq. (31).

In order to obtain the geometrical properties required in the MW equation of state (i.e., B_2 and v_{mol} for MW1; v_{mol} and s_{mol} for MW2), one needs to make thermal averages of such properties over all possible molecular conformations. In principle, this would require rather complicated integration. However, the intramolecular potential restricts the values of the torsional degrees of freedom to very narrow regions. In accordance with the rotational isomeric state approximation (RIS), we can therefore, consider that each torsional degree of freedom adopts either of three possible discrete states, known as t, g^+, and g^-.[53] The number of possible states in the molecule is then 3^ν, where ν is the total number of torsional degrees of freedom. For alkanes of up to eight carbon atoms, the total number of possible states is then not larger than 243, so that the geometrical properties may be determined as an exhaustive Boltzmann average over all the possible states. For larger chains, the averages require use of a Monte Carlo sampling procedure. Both of these two possibilities have been considered in detail elsewhere, and we refer the reader to those papers for further explanations.[18,62]

V. RESULTS AND DISCUSSION

A. Results for model alkanes

Note that all of the interaction sites are hard spheres but the model is not athermal due to the torsional potential. All of the simulations considered in this section were obtained at $T = 366.88$ K. In Table III we present the geometrical parameters required in the MW EOS for several isomers of hexane, heptane, and octane. α^{MW1} stands for the nonsphericity parameter when defined as in Eq. (29) and determined by means of the CBG method, while α^{MW2} is the nonsphericity parameter when defined as in Eq. (31). Within a given group of isomers, both α^{MW1} and α^{MW2} show similar trends, gradually decreasing as the number of branches increases. Obviously, as the interaction sites of an *n*-alkane are removed from the ends and placed closed to the center we might expect that the molecules become more spherical, and the decrease in the nonsphericity parameter reflects this fact. Note, however that α^{MW1} seems to be more sensitive to the molecular shape than α^{MW2} as it takes larger values for the more anisotropic values, and smaller values for the more spherical ones. As an example, consider the octane isomers, where it is seen that the values of α^{MW1} range from 1.578 for *n*-octane, to 1.236 for 2,2,3,3-tetramethylbutane; on the other hand, the corresponding values for α^{MW2} range from 1.517 to 1.340. At any rate the variations of α^{MW1} and α^{MW2} within a group of isomers is always much larger than that shown by the molecular volume, which is seen to change not

TABLE III. Parameters required for the evaluation of the MW equation of state at $T = 366.88$ K. α^{exct} is the nonsphericity parameter as defined from MW1 [Eq. (29)] and determined from the exact second virial coefficient. α^{mw1} is the nonsphericity parameter as defined from MW1 and determined from the methodology proposed in Refs. 18 and 62. α^{mw2} is the nonsphericity parameter as defined from MW2 [Eq. (31)]. v_{mol} is the molecular volume in units of the hard-sphere diameter.

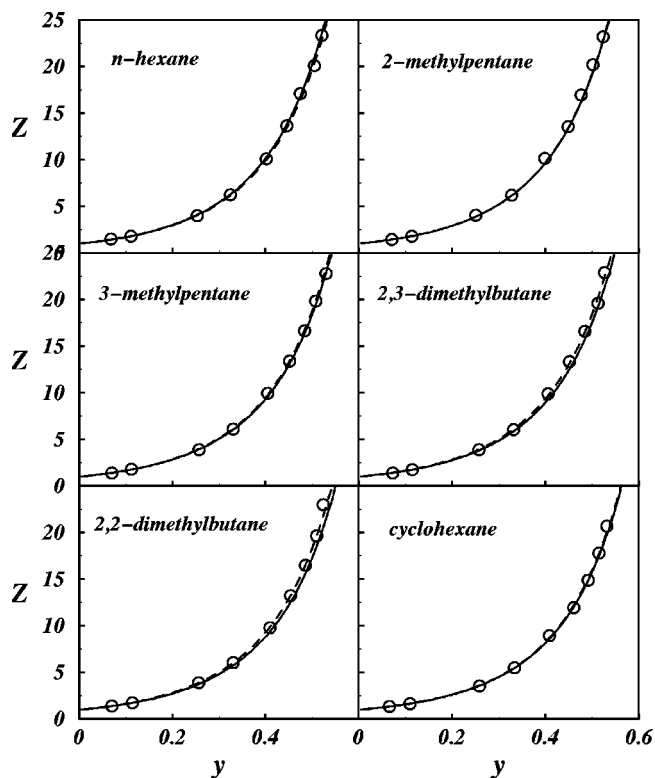| Alkane	α^{exct}	α^{mw1}	α^{mw2}	v_{mol}/d^3
	Hexane isomers			
n-hexane	1.388 764	1.384 190	1.353 67	2.027 161
2-methylpentane	1.342 432	1.326 175	1.331 79	2.020 609
3-methylpentane	1.299 319	1.286 616	1.309 04	2.014 426
2,3-dimethylbutane	1.260 096	1.242 015	1.289 64	2.008 400
2,2-dimethylbutane	1.244 580	1.228 991	1.283 58	2.006 021
cyclohexane	1.148 527	1.147 430	1.159 66	1.832 725
	Heptane isomers			
n-heptane	1.481 831	1.474 216	1.4351	2.326 571
3-methylhexane	1.400 875	1.381 213	1.395 59	2.314 944
3-ethylpentane	1.365 731	1.344 971	1.379 17	2.310 332
2,3-dimethylpentane(R)	1.324 803	1.303 196	1.356 53	2.303 199
3,3-dimethylpentane	1.278 768	1.264 449	1.330 16	2.294 881
2,2,3-trimethylbutane	1.255 534	1.233 229	1.316 36	2.290 177
	Octane isomers			
n-octane	1.573 728	1.578 162	1.517 28	2.625 892
4-methylheptane	1.507 777	1.489 392	1.4845	2.615 952
3-ethylhexane	1.469 124	1.449 776	1.467 49	2.611 095
2,5-dimethylhexane	1.460 839	1.448 761	1.468 14	2.610 603
2,2,3-trimethylpentane(S)	1.324 832	1.309 049	1.3856	2.584 962
3-ethyl-3-methylpentane	1.318 695	1.313 148	1.379 36	2.583 754
2,2,3,3-tetramethylbutane	1.250 243	1.236 054	1.339 63	2.569 577

FIG. 3. Compressibility factors of hexane isomers as a function of the packing fraction. Symbols are results from NpT MC simulations of this work, while the lines are predictions from MW1 (full line) and MW2 (dashed line). Note that packing fractions may be converted back to densities using the molecular volumes of Table III.

more than 2% (with the exception of cyclohexane which is not really a n-hexane isomer in the sense that it has a different chemical formula).

The fact that volume changes are much smaller than nonsphericity changes in our alkane models is quite interesting because it will allow us to discuss the variation of the EOS of the isomers as a function of the molecular anisotropy alone.

As a final point, Table III shows the nonsphericity parameter as defined from Eq. (29) when determined exactly from the true second virial coefficients of the molecules. Note that α^{exact} may only be compared with α^{MW1}, as α^{MW2} has a different definition. What is seen by comparing α^{exact} with α^{MW1} is that the CBG method proposed does give indeed very good and reliable estimates for α^{exact} and so for the second virial coefficient of the molecules. This good agreement was already observed in a previous paper.[62]

Let us now consider the EOS of several different isomers of the alkane series. In Fig. 3 we show the EOS of all the hexane isomers, i.e., n-hexane, 2-methylpentane, 3-methylpentane, 2,3-dimethylbutane, and 2,2-dimethylbutane, as well as that of cyclohexane. The symbols are the results as obtained from simulation, while the full lines are the predictions from MW1 and the dashed line those from MW2. Note that for n-hexane and the two methylpentanes both MW1 and MW2 show excellent agreement with simulation. For 2,3 and 2,2 dimethylbutane the agreement between theory and simulation is also very good, although some differences between MW1 and MW2 become apparent. Finally, the predictions for cyclohexane are seen to

be once more very good. Note, however, that cyclohexane departs somewhat from the previous models because we have considered it a rigid molecule in the chair configuration.[49]

Figure 4 shows the EOS of the heptane isomers. Note that, as the chain length increases, the number of possible isomers increases dramatically and here we consider six out of the nine possible isomers. Our choice is such, however, that we consider all of the possible architectures: The linear isomer, n-heptane; the only isomer with an ethyl group, 3-ethyl-pentane; one out of the two isomers with a single methyl group, 3-methylethane; two out of the four dimethyl isomers, 2,3-dimethylpentane, and 3,3-dimethylpentane; and finally, the most highly branched isomer, 2,2,3-trimethylbutane. Once more, both MW1 and MW2 are seen to be in very good agreement with the simulation results. However, it seems that MW1 slightly underestimates the EOS of the more branched isomers, while MW2 shows here very good predictions for all of the isomers.

When it comes to the octane isomers, there are a total of 18, and here we just consider six representative members: the linear isomer, n-octane; one ethyl isomer, 3-ethylhexane; one methyl isomer, 4-methylheptane; one of the dimethyl isomers, 2,5-dimethylhexane; one methyl-ethyl isomer, 3,3-ethylmethylpentane; and finally the more branched isomer 2,2,3,3-tetramethylbutane. The theoretical prediction for these isomers are shown in Fig. 5. For the first four isomers considered, the agreement between theory and simulation is
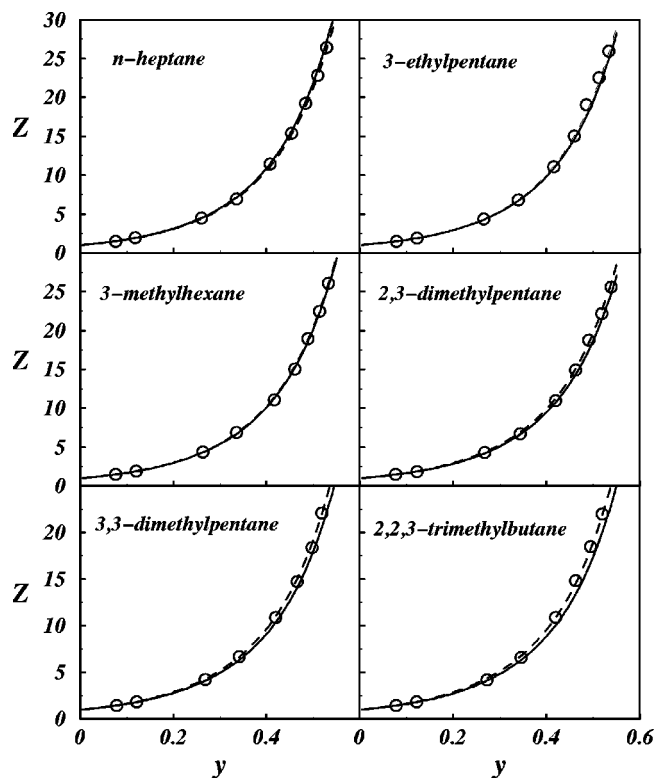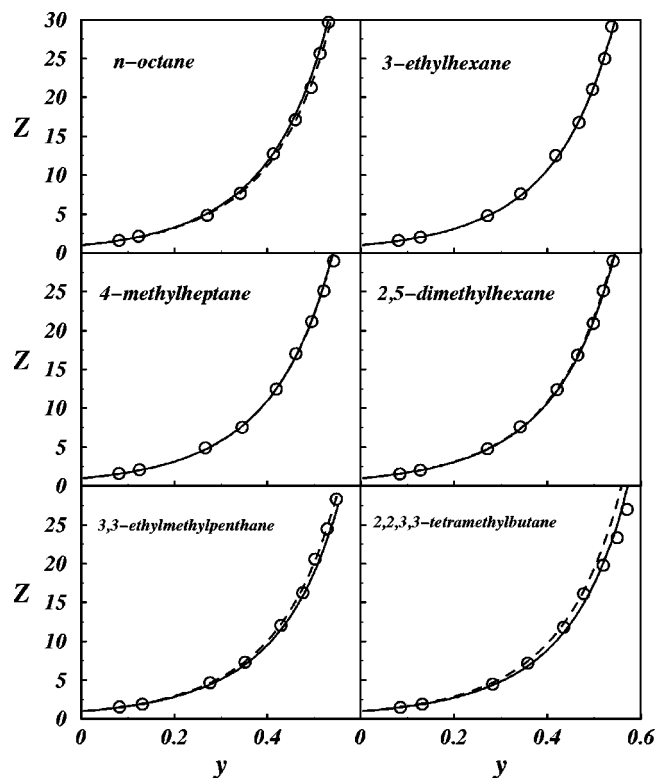
FIG. 4. As in Fig. 3 but for heptane isomers.

FIG. 5. As in Fig. 3 but for octane isomers.

seen to be excellent and the results for MW1 and MW2 are hardly distinguishable. For the two remaining isomers, differences between MW1 and MW2 become apparent, with MW2 predicting somewhat higher compressibility factors than MW1. Overall, both MW1 and MW2 are shown to give rather reliable predictions for the compressibility factor, despite the fact that we have considered a rather broad range of packing fractions, from $y=0$ to $y=0.5$, close to the expected fluid–solid transition.[58]

An interesting issue that was not possible to consider by examining Figs. 3–5 is to what extent do the compressibility factors of the isomers of a given alkane differ. Actually, the differences are rather small and would have hardly been appreciated if plotted in the same graph. For this reason, it proves more convenient to consider Tables IV–VI, which show the simulation results for the isomers of hexane, hep-

tane and octane. To be specific, let us consider Table V, where the EOS of heptane isomers is shown. What is clearly made apparent at first sight, by horizontal inspection of the table is that indeed the EOS of the different isomers is very similar. Comparing pairs of contiguous columns, such as that of 2,3-dimethylpentane (ρ_3) and 3-ethylpentane (ρ_4), it would seem that the EOS is identical within simulation error. The great similarity between the EOS of isomers of repulsive alkanes was already observed by Sear et al. for models made of tangent spheres.[64] A closer inspection at Table V, however, will show interesting systematic trends which are in fact predicted by both MW1 and MW2. Indeed, by taking a look at Eq. (28) one concludes that, for a given pressure, the smaller the nonsphericity, the larger the packing fraction. Accordingly, if the molecular volumes are constant or nearly so, the larger is α the smaller the density. To test this prediction,

TABLE IV. Equation of state of hexane isomers at $T=366.88$ K as obtained from simulation. The pressure, p/k_BT, is given in units of d^3, as well as the densities. From left to right, cyclohexane (ρ_1), 2,2-dimethylbutane (ρ_2), 2,3-dimethyllbutane (ρ_3), 3-methylpentane (ρ_4), 2-methylpentane (ρ_5), and n-hexane (ρ_6). The numbers in parenthesis are a measure of the error in the last digit as measured by a single standard deviation.

p/k_BT	ρ_1	ρ_2	ρ_3	ρ_4	ρ_5	ρ_6
0.05	0.036(3)	0.035(2)	0.036(2)	0.035(3)	0.035(2)	0.034(2)
0.10	0.060(3)	0.057(3)	0.057(3)	0.056(3)	0.056(3)	0.055(3)
0.50	0.141(4)	0.128(3)	0.128(3)	0.128(3)	0.124(5)	0.125(4)
1.00	0.182(4)	0.165(4)	0.165(3)	0.164(4)	0.162(3)	0.160(4)
2.00	0.223(4)	0.204(4)	0.202(4)	0.201(3)	0.197(3)	0.198(3)
3.00	0.251(3)	0.226(3)	0.225(3)	0.224(2)	0.222(3)	0.220(2)
4.00	0.268(3)	0.242(3)	0.241(4)	0.240(2)	0.236(3)	0.234(2)
5.00	0.281(3)	0.254(3)	0.255(2)	0.252(3)	0.248(3)	0.249(2)
6.00	0.290(2)	0.261(2)	0.262(2)	0.263(3)	0.259(2)	0.257(1)

J. Chem. Phys., Vol. 115, No. 13, 1 October 2001

Equation of state of model branched alkanes   6231

TABLE V. Equation of state of heptane isomers. The densities are, from left to right, 2,2,3-trimethylbutane (ρ_1), 3,3-dimethylpentane (ρ_2), 2,3-dimethylpentane (ρ_3), 3-ethylpentane (ρ_4), 3-methylhexane (ρ_5), and n-heptane (ρ_6). Rest of notation as in Table IV.

p/k_BT	ρ_1	ρ_2	ρ_3	ρ_4	ρ_5	ρ_6
0.05	0.034(2)	0.034(2)	0.033(2)	0.034(2)	0.033(2)	0.033(2)
0.10	0.053(3)	0.053(3)	0.053(3)	0.053(3)	0.052(2)	0.051(3)
0.50	0.119(3)	0.117(4)	0.116(4)	0.115(3)	0.114(3)	0.112(3)
1.00	0.151(3)	0.149(3)	0.149(3)	0.147(3)	0.145(3)	0.144(3)
2.00	0.183(2)	0.183(2)	0.182(2)	0.180(2)	0.180(2)	0.175(2)
3.00	0.202(2)	0.203(3)	0.201(2)	0.199(2)	0.199(1)	0.195(2)
4.00	0.216(2)	0.217(3)	0.213(2)	0.210(2)	0.211(2)	0.208(2)
5.00	0.227(2)	0.226(2)	0.225(2)	0.222(1)	0.222(2)	0.219(1)
6.00	0.237(1)	0.234(2)	0.234(2)	0.231(2)	0.230(1)	0.227(2)

Table V collects the EOS of heptane isomers, arranged in columns from the isomer with smaller α (left), to the isomer with higher α (right). Inspection of the last row of this table, where the differences are more apparent, shows that indeed the larger the nonsphericity, the smaller the density at a fixed pressure. What we can conclude from these considerations is that MW1 and MW2 are not only able to give good quantitative predictions for the EOS. They are also able to describe very fine differences that are found between the different isomer of a given alkane.

B. Results for chains with different bond lengths

Previously, we have seen that both MW1 and MW2 are able to correctly estimate the equation of state of a large number of branched alkanes. Here we will consider whether these equations of state may be also applied to other models with larger bond lengths. To this end, we have performed simulations for athermal linear alkanes with $n = 16$. The bond angles are set again to the tetrahedral value, but the torsional potential allows for a free rotation about the bond vectors (i.e., uniform torsional potential). Four different bond lengths l_0/d are considered, namely, $l_0/d = 0.4, 0.6, 0.8, 1$.

In Table VII we collect the molecular parameters required to apply MW1 and MW2. The results obtained from simulation are collected in Table VIII. Comparison with the theoretical equations of state may be seen in Fig. 6, where the pressure ($\rho d^3/k_BT$) is plotted as a function of the number density, ρd^3. For the smallest bond length, $l_0/d = 0.4$, the figure shows that both MW1 and MW2 yield very good

agreement. For larger bond lengths (0.8 and 1.0) MW1 fails clearly, while MW2 in seen to be significantly better, yielding rather reasonable results.

The reason for the discrepancy between MW1 and MW2 at long bond distances may be traced back to the definition of the effective number of tangent hard spheres. In both MW1 and MW2, $n_{ef} = 2\alpha - 1$. By construction, MW2 yields $n_{ef} = n$ in the limit where $l_0 = d$, so that one recovers the original TPT1 result of Wertheim, which is known to be quite accurate. On the other hand, using the definition of α proposed in MW1, one finds that n_{ef} is significantly smaller than n for $l_0 = d$.

It would appear that MW1 is a good equation of state for molecules with bond lengths between 0.4 and 0.6, but that cannot be used for larger bond lengths. Although we have shown that MW1 gives good results for alkanes of up to 30 carbon atoms,[18] a scaling argument shows that it should eventually fail for larger model alkanes. Indeed, it may be shown that MW1 predicts a compressibility factor that scales as $n^{3\nu-1}$, where ν is the exponent for the scaling law of the radius of gyration.[62,65] For repulsive chains, we expect this exponent to be $\nu = 0.6$, so that the compressibility factor is predicted to scale as $n^{0.8}$. On the contrary, it is expected that the compressibility factor of large chain molecules will scale linearly with n,[66] so that MW1 must eventually fail for long enough model alkanes. Despite of this failure, it is expected that MW1 will give better results than MW2 at low densities, as it introduces the exact second virial coefficient by construction. On the other hand, MW2 does not predict the cor-

TABLE VI. Equation of state of octane isomers. The densities are, from left to right, 2,2,3,3-tetramethylbutane (ρ_1), 3-ethyl-3-methylpentane (ρ_2), 2,5-dimethylhexane (ρ_3), 3-ethylhexane (ρ_4), 4-methylheptane (ρ_5), and n-octane (ρ_6). Rest of the notation as in Table IV.

p/k_BT	ρ_1	ρ_2	ρ_3	ρ_4	ρ_5	ρ_6
0.05	0.033(2)	0.032(2)	0.032(2)	0.031(2)	0.031(2)	0.031(2)
0.10	0.051(3)	0.051(2)	0.049(3)	0.049(3)	0.048(2)	0.047(2)
0.50	0.110(4)	0.107(3)	0.104(3)	0.104(3)	0.102(2)	0.103(2)
1.00	0.139(3)	0.136(3)	0.131(2)	0.131(3)	0.132(2)	0.130(2)
2.00	0.169(3)	0.166(2)	0.161(2)	0.160(2)	0.160(3)	0.157(2)
3.00	0.186(2)	0.184(2)	0.178(2)	0.179(2)	0.176(2)	0.175(1)
4.00	0.202(2)	0.194(2)	0.191(2)	0.190(1)	0.189(1)	0.188(2)
5.00	0.214(2)	0.204(1)	0.199(1)	0.200(2)	0.199(2)	0.195(2)
6.00	0.222(2)	0.212(2)	0.207(2)	0.206(1)	0.207(2)	0.202(1)

TABLE VII. Molecular parameters for use in the MW1 and MW2 equations of state for linear chains with 16 monomers as a function of the bond length, l_0. Rest of the caption as in Table III.

l_0/d	α^{exct}	α^{mw1}	α^{mw2}	v_{mol}/d^3
0.4	1.932	2.044	2.0183	4.8311
0.6	2.741	3.040	3.4930	6.7439
0.8	3.86	4.165	5.2805	7.9380
1.0	5.65	5.910	8.5000	8.3776

rect virial coefficients and we have observed that indeed yields worse results than MW1 at low densities.[55] Actually, MW2 and TPT1 are identical for $l=1$ and it has been recently shown that TPT1 produces rather inaccurate virial coefficients.[65]

It is interesting to consider the compressibility factors for $l_0/d=1.0$. For this elongation MW2 reduces to TPT1, which is known to predict accurately the equation of state of the fully flexible pearl-necklace model.[5] However, as seen, in Fig. 5, MW2 (i.e., TPT1) deviates significantly from the simulation results for the tangent sphere model considered in this work. Clearly, the discrepancy is due to the fixed bond angle, which is seen to have a negligible effect at low density, but a very significant one at higher densities. Actually, the pearl necklace model is known to have a crystal phase with closed packed face-centered-cubic (fcc) arrangement of monomers.[67,68] However, fixing the bond angle to the tetrahedral value prevents the formation of a closed packed crystal and freezing thus takes place at much lower densities.[58] Here we observe that the liquid phase already ''feels'' this steric hindrance, which is reflected from the divergence of the compressibility factor.

TABLE VIII. Equation of state results for the athermal alkane model with 16 monomers as obtained from simulation. ρ_1, densities for $l_0=0.6d$; ρ_2, densities for $l_0=0.8d$; ρ_3, densities for $l_0=1.0d$. The results for $l_0=0.4d$ are not included, as they agree with the results of Yethiraj (Ref. 70) within statistical accuracy. We supplement that data set with the state point $(p/k_BT=3.45, \rho=0.102)$. Pressure and density given in units of d^3.

p/k_BT	ρ_1	ρ_2	ρ_3
0.010	0.0066	0.0058	0.0050
0.025	0.0119	0.0098	0.0083
0.050	0.0174	0.0139	0.0115
0.100	0.0237	0.0187	0.0152
0.500	0.0431	0.0332	0.0273
1.000	0.0526	0.0404	0.0338
2.000	0.0626	0.0487	0.0412
3.000	0.0686	0.0534	0.0458
4.000	0.0728	0.0569	0.0488
5.000	0.0761	0.0596	0.0503
6.000	0.0790	0.0615	0.0513
8.000		0.0635	0.0522
10.00		0.0644	0.0526
12.00		0.0651	0.0528
16.00		0.0659	0.0531
20.00		0.0662	0.0533
24.00			0.0534

VI. CONCLUSIONS

In this paper we have considered the statistical thermodynamics of model branched alkanes. We start with a rather realistic Hamiltonian that contains bending and torsional potentials, as well as excluded volume interactions. We show that within the classical flexible constraint approximation, the configurational integral takes a simple form, namely, an integral of the Boltzmann factor of the remaining soft potentials. This follows from the fact that the Jacobian of the transformation form Cartesian to generalized coordinates does not depend on the soft degrees of freedom.

We have then performed configurational bias simulations of several isomers of hexane, heptane, and octane. We find that, provided that the molecular volume of the isomers is similar, the equation of state changes but little. At any rate, the change is such that, at a given packing fraction, the larger the nonsphericity, the larger the pressure. Or, alternatively, at a given pressure, the larger the nonsphericity, the smaller the corresponding equilibrium density.

We have tested two empirical modifications of Wertheim's TPT1 for the prediction of the equation of state. One of these introduces an effective number of tangent hard spheres determined so as to reproduce the exact second virial coefficient of the model (MW1). The other, proposed by Zhow, Hall, and Stell,[16] uses an effective number of spheres such that both molecular surface and volume of the model are reproduced (MW2). We find that both MW1 and MW2 provide a rather satisfactory agreement with simulations, although MW2 has the advantage of being somewhat less computationally demanding. We have also studied the performance of these two equations of state as the bond length changes. We find that MW2 gives rather good results for all reduced bond lengths between 0.4 and 1.0, while MW1 fails for reduced bond lengths larger than 0.6.

As an example of the usefulness of having an accurate equation of state for repulsive molecular models, let us con-
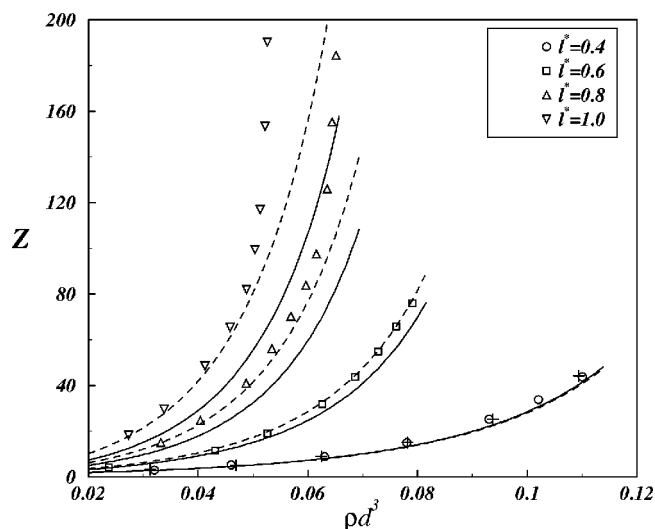

FIG. 6. Compressibility factor for linear chains of 16 atoms and varying bond lengths. Empty symbols are simulation results from this work. The crosses are simulation results from Yethiraj[70] for the same model and $l=0.4$. The full lines are predictions from MW1 while the dashed lines are predictions from MW2.

TABLE IX. Dependence of the critical properties with the molecular parameters as predicted from Eqs. (33)–(35). ↗ and ↘ indicate increase or decrease of the critical property with respect to an increase of the corresponding molecular parameter, respectively. — indicates no effect of the molecular parameter on the critical property.

Critical property	Molecular parameter		
	α	v_{mol}	a_{vdw}
V_c	↗	↗	—
T_c	↘	↘	↗
p_c	↘	↘	↗
Z_c	↘	—	—

sider a simple perturbation theory. Within the spirit of a van der Waals (vdW) theory, we consider the MW form of the equation of state and then add to this a simple mean-field perturbation term. The pressure then takes the form

$$p = p_{MW}(\rho; v_{mol}, \alpha) - a_{vdw}\rho^2, \qquad (32)$$

where p_{MW} is the pressure as predicted by the MW equation of state. If we then apply the conditions for the critical point, we find that the critical properties may be obtained in close form in terms of three molecular parameters, namely, v_{mol}, the molecular volume, α, the nonsphericity, and a_{vdw}, the van der Waals constant.

$$V_c = v_{mol} V_c^*(\alpha), \qquad (33)$$

$$T_c = \frac{a_{vdw}}{k_B v_{mol}} T_c^*(\alpha), \qquad (34)$$

$$p_c = \frac{a_{vdw}}{v_{mol}^2} p_c^*(\alpha), \qquad (35)$$

where V_c^*, T_c^*, and p_c^* are all dimensionless, universal functions of α. The explicit form of these functions is not important. What matters is that V_c^* is a monotonously increasing function of α, while T_c^* and p_c^* are both monotonously decreasing functions of α. This knowledge is enough

to use Eqs. (33)–(35) to make simple qualitative predictions on the variation of the critical properties in terms of the molecular parameters. As an example, Eq. (34) shows that the smaller α, the larger T_c. This explains why highly branched alkanes such as 2,3,3,-trimethyloctane may have a larger critical temperature than n-octane, when it is expected that the former should have a smaller van der Waals constant.

Equations (33)–(35) may be considered as a succinct rationalization of the results we obtained in a previous paper, where we found that a mean-field theory could qualitatively predict the critical properties of branched alkanes.[28] Table IX presents a summary of the conclusions drawn form these equations.

ACKNOWLEDGMENTS

APPENDIX A: JACOBIAN OF THE TRANSFORMATION FROM CARTESIAN TO GENERALIZED COORDINATES IN BRANCHED ALKANES

In this Appendix we show that the Hamiltonian of the transformation from Cartesian coordinates to generalized coordinates in a branched alkane is independent of the torsional degrees of freedom, $\{\phi\}$.

Consider a small fragment of some arbitrary branched alkane, as shown in Fig. 7. This fragment is made of a linear chain of atoms $i-3$, $i-2$, $i-1$, i. Now, let there be two branched atoms, $i+1$ and $i+2$ bonded to atom $i-1$. Let the
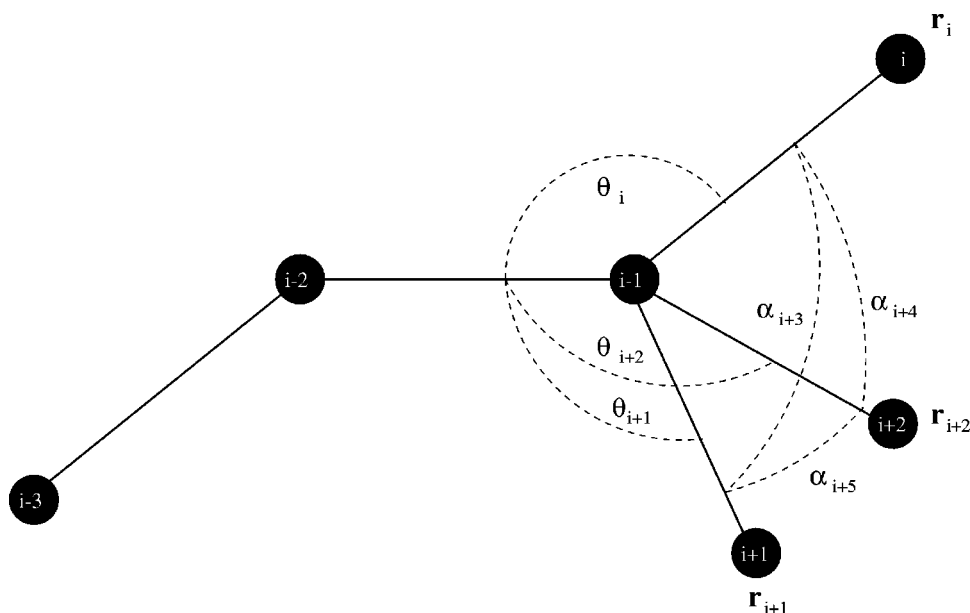

FIG. 7. Sketch of a branched alkane. θ_i, θ_{i+1}, and θ_{i+3} define bond angles formed between atoms i, $i+1$, and $i+2$ and the backbone. α_{i+3}, α_{i+4}, and α_{i+5} are bond angles formed between the bond vectors $\mathbf{r}_i$, $\mathbf{r}_{i+1}$, and $\mathbf{r}_{i+2}$. φ_i, φ_{i+1}, and φ_{i+2} (not shown) are dihedral angles that describe the orientation of atoms i, $i+1$, and $i+2$ relative to the axis formed between $i-2$ and $i-1$.

set of polar coordinates that specify the position of atom i relative to a reference frame formed from atoms $i-1$, $i-2$ and $i-3$ be l_i, θ_i, and φ_i. Let there be similar sets l_{i+1}, θ_{i+1}, and φ_{i+1} for atom $i+1$ and similarly for atom $i+2$. Note that polar angles θ correspond to bond angles, while azimuthal angles φ correspond to dihedral angles.

Using a local reference frame and an appropriate rotation matrix, the Cartesian coordinates of atoms i, $i+1$ and $i+2$ may be written as:[53]

$$\mathbf{r}_j = l_j(\cos\tilde{\theta}_j, \sin\tilde{\theta}_j\cos\varphi_j, \sin\tilde{\theta}_j\sin\varphi_j), \tag{A1}$$

where $\tilde{\theta}_j$ is the complementary of bond angle θ_j and j ranges from i to $i+2$. The Jacobian of the transformation from Cartesian to polar coordinates for these three atoms may be then shown to be

$$J_{c\to p} = \prod_{j=i}^{i+2} l_j^2 \sin\theta_j. \tag{A2}$$

The Jacobian from Cartesian to polar coordinates for an atom belonging to a linear chain has been already considered by Go and Scheraga.[44] Note that what is obtained here is the product of the Jacobians for the last atom of the three linear sequences $(i-3)-(i-2)-(i-1)-i$, $(i-3)-(i-2)-(i-1)-(i+1)$, and $(i-3)-(i-2)-(i-1)-(i+2)$.

The set of polar coordinates used to describe atoms i, $i+1$, $i+2$ is not convenient, however. The reason is that, owing to the branches new bond angles α_{i+3}, α_{i+4}, and α_{i+5} appear (see Fig. 7). These bond angles have a corresponding hard potential, and it would be desirable to have a set of generalized coordinates that explicitly accounts for them. In order to proceed, we take the scalar products $\mathbf{r}_i \cdot \mathbf{r}_{i+1}$, $\mathbf{r}_i \cdot \mathbf{r}_{i+2}$, $\mathbf{r}_{i+1} \cdot \mathbf{r}_{i+2}$ and obtain

$$\cos\alpha_{i+2+k} = \cos\tilde{\theta}_i\cos\tilde{\theta}_{i+k} + \sin\tilde{\theta}_i\sin\tilde{\theta}_{i+k}\cos\Delta_{i+k}, \tag{A3}$$

$$\cos\alpha_{i+5} = \cos\tilde{\theta}_{i+1}\cos\tilde{\theta}_{i+2} + \sin\tilde{\theta}_{i+1}\sin\tilde{\theta}_{i+2}$$
$$\times\cos(\Delta_{i+1}-\Delta_{i+2}), \tag{A4}$$

where k is either 1 or 2 and $\Delta_{i+k} = \varphi_{i+k} - \varphi_i$.

Note that the set of Eqs. (A3) and (A4) immediately suggest a very convenient new set of coordinates, θ_i, θ_{i+1}, θ_{i+2}, Δ_{i+1}, Δ_{i+2}, φ_i, which completely specify the position of atoms i, $i+1$, and $i+2$. We choose to call these the internal set of coordinates. Note already that with the internal set of coordinates all of the bond angles may be expressed independently of the dihedral angle φ_i. The transformation from polar to internal coordinates is trivial, and the corresponding Jacobian can be seen to be $J_{p\to i}=1$.

These set of coordinates is, however, still nonconvenient, because the bending potentials will become complicated functions of Δ_{i+1}, Δ_{i+2}. For this reason, we choose a set of generalized coordinates, α_i, α_{i+1}, α_{i+2}, α_{i+3}, α_{i+4}, ϕ, made of five of the six bond angles, and one single torsional degree of freedom, ϕ

$$\theta_i = \alpha_i, \tag{A5}$$

$$\theta_{i+1} = \alpha_{i+1}, \tag{A6}$$

$$\theta_{i+2} = \alpha_{i+2}, \tag{A7}$$

$$\Delta_{i+1} = \Delta_{i+1}(\alpha_i, \alpha_{i+1}, \alpha_{i+3}, \phi), \tag{A8}$$

$$\Delta_{i+2} = \Delta_{i+2}(\alpha_i, \alpha_{i+2}, \alpha_{i+4}, \phi), \tag{A9}$$

$$\varphi_i = \phi. \tag{A10}$$

At first instance, it is convenient to write the Jacobian of this transformation formally

$$J_{i\to g} = \begin{vmatrix} 1 & 0 & 0 & 0 & 0 & 0 \\ 0 & 1 & 0 & 0 & 0 & 0 \\ 0 & 0 & 1 & 0 & 0 & 0 \\ \left(\dfrac{\partial\Delta_{i+1}}{\partial\alpha_i}\right) & \left(\dfrac{\partial\Delta_{i+1}}{\partial\alpha_{i+1}}\right) & 0 & \left(\dfrac{\partial\Delta_{i+1}}{\partial\alpha_{i+3}}\right) & 0 & \left(\dfrac{\partial\Delta_{i+1}}{\partial\phi}\right) \\ \left(\dfrac{\partial\Delta_{i+2}}{\partial\alpha_i}\right) & 0 & \left(\dfrac{\partial\Delta_{i+2}}{\partial\alpha_{i+2}}\right) & 0 & \left(\dfrac{\partial\Delta_{i+2}}{\partial\alpha_{i+4}}\right) & \left(\dfrac{\partial\Delta_{i+2}}{\partial\phi}\right) \\ 0 & 0 & 0 & 0 & 0 & 1 \end{vmatrix}, \tag{A11}$$

one then gets simply

$$J_{i\to g} = \left(\frac{\partial\Delta_{i+1}}{\partial\alpha_{i+3}}\right)\cdot\left(\frac{\partial\Delta_{i+2}}{\partial\alpha_{i+4}}\right). \tag{A12}$$

The derivatives may be obtained by implicit derivation from Eq. (A3)

$$\left(\frac{\partial\Delta_{i+k}}{\partial\alpha_{i+2+k}}\right) = \frac{\sin\alpha_{i+2+k}}{\sin\alpha_i\sin\alpha_{i+k}\sqrt{1-\cos^2\Delta_{i+k}}}, \tag{A13}$$

where again k is either 1 or 2 and

$$\cos\Delta_{i+k} = \frac{\cos\alpha_{i+2+k} - \cos\alpha_i\cos\alpha_{i+k}}{\sin\alpha_i\sin\alpha_{i+k}}. \tag{A14}$$

Now, the Jacobian of the overall transformation from Cartesian to generalized coordinates is just the product of $J_{c\to p}$, $J_{p\to i}$, $J_{i\to g}$, so that we finally get

$$J_{c\to g} = l_i^2\sin\alpha_i\prod_{k=1}^{2}\left[\frac{l_{i+k}^2\sin\alpha_{i+2+k}}{\sin\alpha_i\sin\Delta_{i+k}}\right]. \tag{A15}$$

It is then seen that $J_{c\to g}$ only depends on the hard bond

angle variables, so that it is explicitly independent of the remaining soft degree of freedom, ϕ, a torsional angle. One can therefore integrate out all of the hard variables in Eq. (7) (not all the integrals over α_i are trivial, however) and this leads to the configuration integral of Eq. (8). Also note that when the bending potential is infinitely stiff, the internal variables Δ_{i+1} and Δ_{i+2} are completely specified by the equilibrium values of the bond angles. The only remaining degree of freedom required to specify the state of atoms i, $i+1$, and $i+2$ is the torsional angle ϕ, while the dihedral angle φ_{i+k} is given by $\varphi_{i+k} = \phi + \Delta_{i+k}$.

In order to obtain the Jacobian of the complete chain, it suffices to substitute the upper limit of the productory of Eq. (A15) by $\eta(i)$, the number of branches of atom i. The complete Jacobian is then obtained as a productory of Eq. (A15) over all the atoms of the chain (less the three first), following a complete growth path as described previously. For atoms with $\eta(i) = 0$, we recover the simple Go–Scheraga term, $l_i^2 \sin(\alpha_i)$, that corresponds to a linear chain.[44] Here we have considered the general case of a branched alkane. Apparently, the less general case of an isobutane fragment has already been considered.[69] Note also that the Jacobian of Eq. (A15) may be useful for effective sampling of bond angles in more detailed models with an explicit bonding potential.

[1] M. S. Wertheim, J. Stat. Phys. **35**, 19 (1984).
[2] M. S. Wertheim, J. Stat. Phys. **35**, 35 (1984).
[3] M. S. Wertheim, J. Stat. Phys. **42**, 459 (1986).
[4] M. S. Wertheim, J. Stat. Phys. **42**, 477 (1986).
[5] M. S. Wertheim, J. Chem. Phys. **87**, 7323 (1987).
[6] R. Dickman and C. K. Hall, J. Chem. Phys. **85**, 4108 (1986).
[7] K. G. Honnell and C. K. Hall, J. Chem. Phys. **90**, 1841 (1989).
[8] L. Lue, J. Chem. Phys. **112**, 3442 (2000).
[9] W. G. Chapman, G. Jackson, and K. E. Gubbins, Mol. Phys. **65**, 1057 (1988).
[10] A. Yethiraj and C. K. Hall, J. Chem. Phys. **94**, 3943 (1991).
[11] C. S. Patrickios and L. Lue, J. Chem. Phys. **113**, 5485 (2000).
[12] T. Boublik, C. Vega, and M. Diaz-Peña, J. Chem. Phys. **93**, 730 (1990).
[13] J. M. Walsh and K. E. Gubbins, J. Phys. Chem. **94**, 5115 (1990).
[14] M. D. Amos and G. Jackson, J. Chem. Phys. **96**, 4604 (1992).
[15] S. Phan, E. Kierlik, and M. L. Rosinberg, J. Chem. Phys. **101**, 7997 (1994).
[16] Y. Zhou, C. K. Hall, and G. Stell, J. Chem. Phys. **103**, 2688 (1995).
[17] C. Vega, S. Lago, and B. Garzon, J. Chem. Phys. **100**, 2182 (1994).
[18] C. Vega, L. G. MacDowell, and P. Padilla, J. Chem. Phys. **104**, 701 (1996).
[19] C. Vega, B. Garzón, L. G. MacDowell, P. Padilla, S. Calero, and S. Lago, J. Phys.: Condens. Matter **8**, 9643 (1996).
[20] A. Yethiraj, J. G. Curro, K. S. Schweizer, and J. D. McCoy, J. Chem. Phys. **98**, 1635 (1993).
[21] L. A. Costa, Y. Zhou, C. K. Hall, and S. Carra, J. Chem. Phys. **102**, 6212 (1995).
[22] S. D. Mehta and K. G. Honnell, Mol. Phys. **96**, 1285 (1996).
[23] E. Enciso, J. Alonso, N. G. Almarza, and F. J. Bermejo, J. Chem. Phys. **90**, 413 (1989).
[24] E. Enciso, J. Alonso, N. G. Almarza, and F. J. Bermejo, J. Chem. Phys. **90**, 422 (1989).
[25] J. Pavlicek and T. Boublik, J. Phys. Chem. **96**, 2298 (1992).
[26] J. Pavlicek, K. Aim, and T. Boublik J. Phys. Chem. **99**, 15662 (1995).
[27] C. Vega and L. G. MacDowell, Mol. Phys. **88**, 1575 (1996).
[28] L. G. MacDowell and C. Vega, J. Chem. Phys. **109**, 5681 (1998).

[29] I. V. Makeeva, S. K. Talitskikh, and P. G. Khalatur, Russ. J. Phys. Chem. **75**, 32 (2001).
[30] W. L. Jorgensen, J. D. Madura, and C. J. Swenson, J. Am. Chem. Soc. **106**, 6638 (1984).
[31] M. J. Dijkstra, J. Chem. Phys. **107**, 3277 (1997).
[32] M. D. Macedonia and E. J. Maginn, Mol. Phys. **96**, 1375 (1999).
[33] M. G. Martin and J. I. Siepmann, J. Phys. Chem. B **103**, 4508 (1999), and references therein.
[34] T. J. H. Vlugt, R. Krishna, and B. Smit, J. Phys. Chem. B **103**, 1102 (1999), and references therein.
[35] N. G. Almarza, E. Enciso, J. Alonso, F. J. Bermejo, and M. Álvarez, Mol. Phys. **70**, 485 (1990).
[36] J. I. Siepmann and D. Frenkel, Mol. Phys. **75**, 59 (1992).
[37] J. J. de Pablo, M. Laso, and U. W. Suter, J. Chem. Phys. **96**, 2395 (1992).
[38] D. Frenkel, G. C. A. M. Mooij, and B. Smit, J. Phys.: Condens. Matter **3**, 3053 (1991).
[39] M. Laso, J. J. de Pablo, and U. W. Suter, J. Chem. Phys. **97**, 2817 (1992).
[40] B. Smit, S. Karaborni, and J. I. Siepmann, J. Chem. Phys. **102**, 2126 (1995); erratum: J. Chem. Phys. **109**, 352 (1998).
[41] J. J. Potoff, J. R. Errington, and A. Z. Panagiotopoulos, Mol. Phys. **97**, 1073 (1999).
[42] P. Ungerer, C. Beauvais, J. Delhommelle, A. Boutin, B. Rousseau, and A. Fuchs, J. Chem. Phys. **112**, 5499 (2000).
[43] J.-P. Ryckaert and A. Bellemans, Chem. Soc. Faraday Discussions **66**, 95 (1978).
[44] N. Go and H. A. Scheraga, Macromolecules **9**, 535 (1976).
[45] M. H. Kalos and P. A. Whitlock, *Monte Carlo Methods* (Wiley, New York, 1986), Vol. 1.
[46] E. J. Maginn, A. T. Bell, and D. N. Theodorou, J. Phys. Chem. **99**, 2057 (1995).
[47] Y. Iba, (2000), cond-mat/0012323.
[48] D. Frenkel and B. Smit, *Understanding Molecular Simulation* (Academic, San Diego, 1996).
[49] R. T. Morrison and R. N. Boyd, *Organic Chemistry*, 5th ed. (Allyn and Bacon, Boston, 1987).
[50] "If one thinks of a branched alkane as a phylogenic tree, the order is equivalent to the number of generations of the tree."
[51] "An alternative method for the selection of growing paths has also been suggested by Martin and Siepman" (Ref. 33).
[52] M. Allen and D. Tildesley, *Computer Simulation of Liquids* (Clarendon, Oxford, 1987).
[53] P. J. Flory, *Statistical Mechanics of Chain Molecules* (Wiley, New York, 1969).
[54] W. H. Press, S. A. Teukolsky, W. T. Vetterling, and B. P. Flannery, *Numerical Recipes in Fortran*, 2nd ed. (Cambridge University Press, Cambridge, 1992).
[55] L. G. MacDowell, Ph.D. thesis, Universidad Complutense de Madrid, 2000.
[56] A. Poncela, A. M. Rubio, and J. J. Freire, Mol. Phys. **91**, 189 (1997).
[57] J. L. F. Abascal and F. Bresme, Mol. Phys. **76**, 1411 (1992).
[58] A. P. Malanoski and P. A. Monson, J. Chem. Phys. **110**, 664 (1999).
[59] N. Almarza (private communication).
[60] N. G. Almarza, E. Enciso, and F. J. Bermejo, J. Chem. Phys. **96**, 4625 (1992).
[61] M. S. Wertheim, J. Chem. Phys. **85**, 2929 (1986).
[62] L. G. MacDowell and C. Vega, J. Chem. Phys. **109**, 5670 (1998).
[63] L. R. Dodd and D. N. Theodorou, Mol. Phys. **72**, 1313 (1991).
[64] R. P. Sear, M. D. Amos, and G. Jackson, Mol. Phys. **80**, 777 (1993).
[65] C. Vega, J. M. Labaig, L. G. MacDowell, and E. Sanz, J. Chem. Phys. **113**, 10398 (2000).
[66] Y. Zhou, S. W. Smith, and C. K. Hall Mol. Phys. **86**, 1157 (1995).
[67] A. P. Malanoski and P. A. Monson, J. Chem. Phys. **107**, 6899 (1997).
[68] C. Vega and L. G. MacDowell, J. Chem. Phys. **114**, 10411 (2001).
[69] M. L. Greenfield, Ph.D. thesis, Department of Chemical Engineering, 1996, according to Ref. 32.
[70] A. Yethiraj, J. Chem. Phys. **102**, 6874 (1995).